Automated Applied Pressure Control for Acoustic Signal Analysis with an Electronic Stethoscope

Jonathan Ims, Samuel Hastings, Eugene Chabot, PhD, and Ying Sun, PhD
Department of Electrical, Computer, and Biomedical Engineering
University of Rhode Island, Kingston, RI 02881-0805 USA

***Abstract*— The ubiquitous stethoscope has been used mainly as a qualitative diagnostic tool. For quantitative analyses, how much pressure applied to the interface between the stethoscope probe and the skin could affect the signal properties such as the frequency spectrum. In this study a device has been developed to control the applied pressure of an electronic stethoscope automatically. An embedded control system ensures that consistent and repeatable acoustic data can be recorded at an optimal pressure. Preliminary results have shown that the device is capable of recording breathing sounds with consistent frequency spectrum over multiple trials. Furthermore, the recorded frequency spectra are sensitive to the applied pressure. Thus, this device should provide a useful tool for quantitative analyses of acoustic signals recorded from the human body.**

***Keywords*— stethoscope; applied pressure; pneumatic control; embedded system; acoustic signal analysis; frequency spectrum**

I. Introduction

One of the on-going research projects at the University of Rhode Island is to study the breathing sounds related to sleep disorders such as obstructive sleep apnea. Sleep apnea is characterized as breaks in the breathing patterns or shallow breaths during sleep [1]. Data suggest that up to 5% of adults are affected by this chronic disease [2]. Current tests for sleep apnea require a patient to stay overnight in a sleep lab and take a sleep test called a polysomnogram. One of the main problems with the polysomnogram is the time required to obtain the data [3]. Thus, our on-going research explores alternative methods such as signal analyses of the breathing sounds recorded with an electronic stethoscope. However, one of the problems that have surfaced is the lack of standardized pressure applied to the stethoscope probe, which could cause significant variations in signal properties.

The system developed in this study utilizes an electronic stethoscope to record the patient's breathing sounds. In order to obtain useful and repeatable data, a constant pressure must be applied to hold and maintain the pressure on the stethoscope probe. An automated applied pressure controller is designed to maintain a preset constant pressure. This paper describes the design and shows preliminary data of frequency spectra of breathing sounds recorded at the suprasentral notch.

II. Methods

A. Design Approach

As shown in Fig. 1, this device was designed to incorporate a constant source of pressure for stabilizing a hands free stethoscope that produces consistency when recording breathing sounds at the suprasentral notch. A harness was developed to allow the stethoscope to be placed within the same region of the body for different patients. Attached to the harness is a neoprene bladder, which is inflated to improve contact between the patient and the stethoscope. The automated pressure system is controlled by an embedded microprocessor (PIC18F4525, Microchip, Chandler, AZ). The processor reads an input voltage from the pressure sensor to and drive a pneumatic pump to inflate or delate the bladder until the desirable applied pressure is reached.

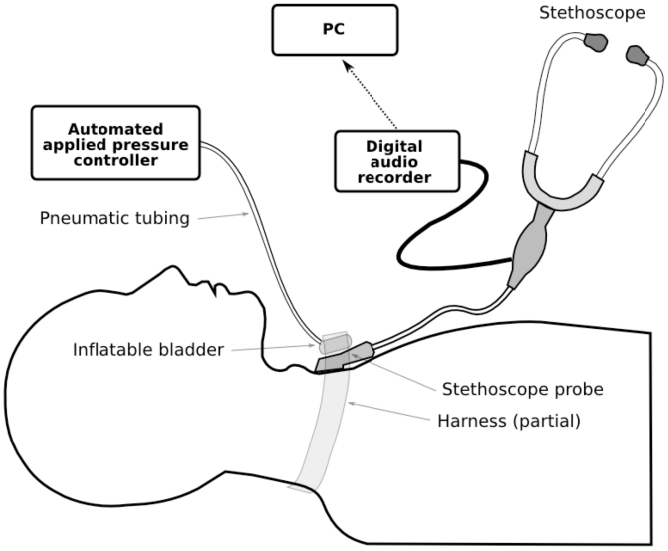

Fig. 1. Schematic diagram of the instrumentation of recording breathing sounds with an automated applied pressure controller.

B. Measurement Harness

The harness is made of several components that were modified to work together. The main component is the *Confor Clavicle Brace*. The brace consists of two shoulder straps that connect around the back and can be adjusted by Velcro. Attached to the brace is a neck strap that includes a buckle and Velcro. The neck strap spans across the patients suprasternal notch to hold the bladder on the stethoscope and to hold the stethoscope in place. The Jabes Electronic Stethoscope is used in conjunction with a H4N digital audio recorder during the test trials to record the breathing sounds. There were three different preset pressures that the bladder was set to. At each pressure breathing sounds were recorded for 20 seconds. There was also a trial conducted holding the stethoscope by hand. These sounds are then analyzed by using MATLAB's fast Fourier transform (FFT) function to determine the frequency spectra. The four different tests trials

were conducted three times to compare for consistency.

C. Automated Pressure Controller

In order to inflate the neoprene bladder, a system controller was developed to apply consistent pressure. With a custom microprocessor circuit, the air pressure is applied via the pump. A release valve is also included in the peumatic system. The valve is a voltage controlled solenoid that closes when a voltage is applied. In order to activate the pump and the valve properly a separate power source was engaged by the system via a MOSFET switch. An air pressure sensor is also utilized on the same tubing to read the back pressure from the bladder. This will give us an estimate of the pressure between the stethoscope and the skin. To adjust the pressure there are 3 push buttons, each with their own function.

The software allows for 3 push button interrupts, a timer interrupt, a display, 2 digital outputs, and an analog input. The primary button's function is to turn the motor on until a preset pressure is achieved. Each time this is pressed it increases to a higher preset pressure (3 levels) until the maximum level is reached. The second button does just the opposite. By pressing the decrease button the solenoid opens until the air pressure is decreased to the level below the current. The third and final valve has 2 functions. The first is an emergency release valve, and the second is to release the pressure after all the tests have been completed. The timer interrupt constantly checks to see if the pressure has reached a critical level (in case of system failure) and will turn the motor off and open the release valve if that level is exceeded.

III. Results

Figure 2 displays the frequency spectra obtained with three different settings: hand held, lowest setting, and highest setting of the automated applied pressure controller. For each setting the recordings were done twice to evaluate their consistency.

IV. Discussion

From Fig. 2, it can be determined that there is consistency in the trials involving the automated pressure device. Each trial was done 3 times and recorded randomly to ensure that there was the data was not skewed. In the hand trials, the spectral analysis shows some variations (arrows in Fig. 2), which is exactly what this project was designed to remove. As for the automated pressure device, it is shown that there is an improved element of consistency when each test is compared. However, on the first test trial there was an interference that came from an electromagnetic hum produced from the wire going to the recording device. By applying an electromagnetic shield, the noise from the source was reduced to a negligible. This design will be integrated into the box when the device is moved from the breadboard onto a protoboard. The first peak in each of the graphs represents an extremely low frequency pulse determined to be the heartbeat of the patient. This leaves the rest of the spectrum to be the different frequencies that make up the breathing sounds.

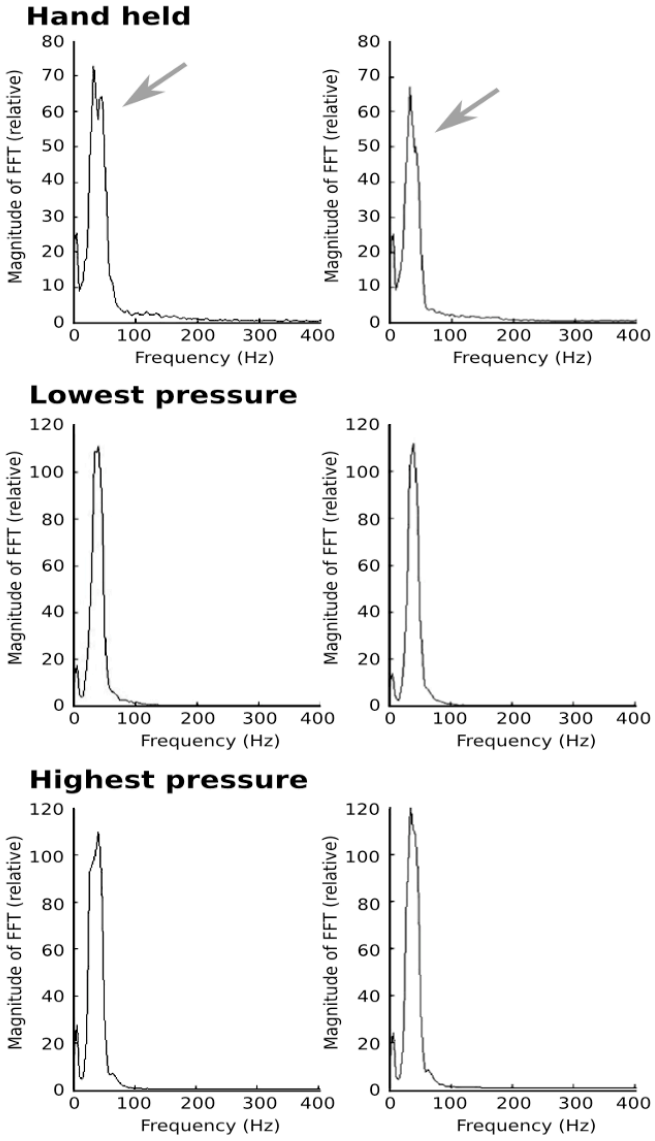

Figure 2: Comparison of two trials for hand held (top), lowest setting (middle) and highest setting (bottom) with the automated controller.

In the future, an IRB approved study will be conducted to provide a formal evaluation of the device with 20 human subjects. Each subject will undergo a hand held and device test. Both body mass and height will be recorded as well, this will help show that the device will give a consistent pressure no matter the BMI of the subject. When all parameters have been determined, the pressure values can be calibrated to improve the next round of trials.

References

[1] G.C. Gutierrez-Tobal, D. Alvarez, J.V. Marcos, F. Del Campo, R. Hornero. Pattern recognition in airflow recordings to assist in the sleep apnoea-hypopnoea syndrome diagnosis. *Med Bio Eng Comput* 51: 1367-1380, 2013.

[2] Staff, Mayo Clinic. Sleep Apnea: Tests and Diagnosis."*Mayo Clinic*. Mayo Foundation for Medical Education and Research, 24 July 2012. Web. 20 Sept. 2013.

[3] K. Johnson. Tests for Diagnosing Sleep Apnea. *WebMD*.Ed. WebMD, June 1, 2012. Web. 20 Sept. 2013.

Graded Muscle Contractions Determined by Temporal Recruitment

Brooke McCarthy, Kimberly Stephens, Caitlyn King, Eugene Chabot, PhD and Ying Sun, PhD

Department of Electrical, Computer, and Biomedical Engineering University of Rhode Island
4 East Alumni Avenue, Kingston, RI 02881-0805, USA

***Abstract*—Electromyogram (EMG) signals have the potential to allow patients without total muscle controls to operate electronic or mechanical devices, such as a power wheelchair. A muscle contraction can be interpreted as a switching signal and its strength can determine the intended level. The purpose of this study is to implement an algorithm to accurately detect the strength of a muscle contraction. Muscle contraction strength can be increased by temporal or spatial recruitment. In this case, the graded muscle contraction is detected by the temporal recruitment, where the frequency of the EMG signal is evaluated. A nonlinear detection algorithm is used to define the duration of a contraction episode. The frequency of the spikes within the contraction episode is used to determine the contraction strength. The algorithm should be useful for designing myoelectrically controlled devices.**

***Keywords*—electromyogram; myoelectric control; graded muscle contraction; temporal recruitment; signal processing; nonlinear detection algorithm**

I. Introduction

Myoelectric controls have been widely used for prosthetics and assistive technology for several decades [1]. However, how to extract the maximum amount of information from the electromyogram (EMG) remains to be an important topic of on-going research. People with limited mobility can benefit from various devices that are operated by interpreting signals from muscle contractions. For example, a power wheelchair has the potential to be completely directed by the contractions of any muscles that produce reliable electrical signals, but not necessarily sufficient mechanical forces [2].

The strength of a muscle contraction can be increased via two types of recruitment: spatial recruitment and temporal recruitment [3]. Spatial recruitment is the increase in number of motor units in order to increase strength. This results in an electromyogram signal with greater amplitude. Temporal recruitment, or rate coding, is the increase in rate of action potentials in order to increase the strength of a contraction [1]. This results in an electromyogram signal with a greater frequency. This study developed a technique to grade muscle contractions into three levels; low, medium, and high. This is accomplished by 1) detecting a time interval of sustained contractions and 2) estimating the frequency of the firing of action potentials and quantifying it to three levels of contraction strength. The project has been implemented on an embedded system platform. The algorithms have been developed and coded in the C language.

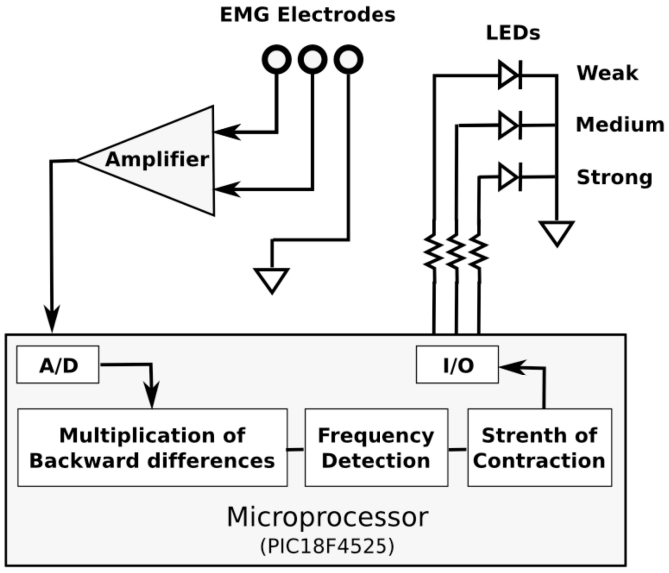

Fig. 1. Block diagram of the embedded system for quantifying the strength of muscle contractions

II. Methods

A. Instrumentation

The embedded system for EMG measurement was based on a previous project [4]. The electromyogram signal was attained by using three surface electrodes places on an individual. Two of electrodes are located on the forearm used to pick the muscle contraction. The third electrode is used a reference (ground) point for voltage. The electrodes are connected to leads that fed into an amplifier. The amplified electromyogram signal are then inputted to a microprocessor (PIC18F4525, Microchip, Chandler, AZ). To distinguish between the outputs from the PIC microprocessor, three LEDs are connected. Each LED corresponds to a different grade that will illuminate when each grade is detected. The different grades are strong, medium, and weak muscle contractions.

B. Peak Detection

The strength of a muscle contraction can be increased by spatial recruitment and by temporal recruitment. It has been proven that temporal recruitment is easier to reconstruct [3]. Using this theory, it is more effective to interpret the strength

of a muscle contraction by finding the frequency of an EMG signal instead of the amplitude of an EMG signal.

In order to detect the EMG signal, the multiplication of backwards differences (MOBD) algorithm was used [5]. The MOBD is an estimate of the derivative of a digital signal. The derivative of the EMG signal allows the peaks to be easily detected. The frequency of the signal is determined by the number of peaks that are detected over a 250 ms window. To determine the MOBD, the current EMG value is subtracted by the previous value. Let d_0 be the current value of the backwards difference.

$$d_0 = emg_0 - emg_1 \quad (1)$$

To detect the peaks of the signal, the absolute values of the current and previous two differences are dividing by eight [1]. Let d_1 and d_2 be the previous values of the backwards difference and M be the current result from the MOBD algorithm.

$$M = \frac{|d_0||d_1||d_2|}{8} \quad (2)$$

C. *Frequency Calculation*

The frequency of the peaks is directly related to the strength of the contraction. The frequencies used to determine the strength of the contraction were theoretically derived. The frequency of the action potentials is directly proportional to the frequency of the EMG signal.

The frequency of activation is estimated within a 250 ms window. The 250 ms window was chosen as a compromise between the robustness of the frequency estimation and the response time of the system. An increase of this time window would increase the robustness but at the sacrifice of slowness of the system's response. Each peak is counted over 250 ms and recorded. The relationship over this time frame allows the program to observe enough to determine the difference between a weak, medium, and strong contraction. A higher frequency corresponds to a stronger muscle contraction.

III. Results

The constructed device was able to execute the accurate detection of a weak, medium, or strong muscle contraction. It determines the frequency of the electromyogram signal and translates it to a grade: weak, medium, or strong. An LED corresponding to a grade illuminates when the different grades are detected. Figure 2 shows a typical result that the user made sequential contractions from weak, to medium and to strong. The LEDs were indicative of the contraction strength.

IV. Discussion

To obtain graded contraction strength from EMG, a technique and device implementing this technique has been developed to estimate the frequency of the muscle contracts instead of measuring the amplitude of the peaks. It has been researched by Safavynia and Ting, who found that measuring the frequency of the peaks rather than the amplitude of S the peaks is a more reliable and accurate depiction of the graded potential [3]. For future work, muscle fatigue should be taken into consideration. Over the course of a muscle contraction, the signal decreases quickly with time due to muscle fatigue. Muscle fatigue is unavoidable and fatigue will alter the results of the graded potential. When the muscle fatigues, the muscle weakens because there are less motor neurons contracting and as a result, the amplitude and the frequency will decrease with time.

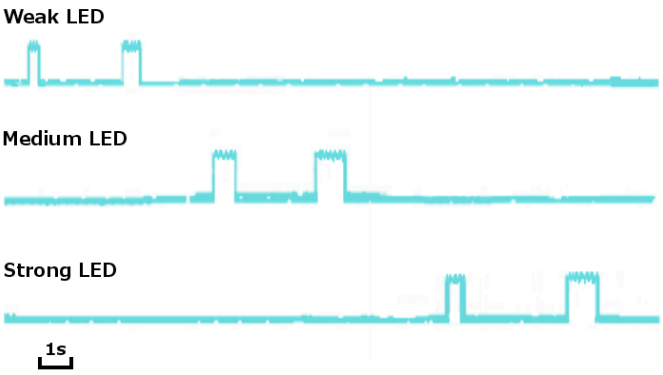

Fig. 2. Oscilloscope display of the on/off signals for the LEDs showing the weak, medium, and strong contractions, as the user sequentially increased the strength of muscle contractions.

The study has demonstrated an effective algorithm for quantifying the muscle contraction strength. The algorithm can be implemented in real time with a low-cost embedded processor. The ability to accurately detect graded muscle contractions can be applied to devices such as powered wheelchairs, prosthetic limbs, as well as other assistive technology devices.

References

[1] F. Sandbrink. Motor unit recruitment in EMG definition of motor unit recruitment and overview. Medspace. June 26. 2012. <http://emedicine.medscape.com/article/1141359-overview>

[2] Sherman, Sheilagh. Sunrise Medical, Canadian Clinical Blog. Pushrim Activated Power Assist Wheelchairs- Clinical Benefits and Considerations. Clinical Corner. September. 2013. <http://www.clinical-corner.com/2013/03/pushrim-activated-power-assist-wheelchairs-clinical-benefits-and-considerations/>

[3] S.A. Safavynia, L.H. Ting. Task-level feedback can explain temporal recruitment of spatially fixed muscle synergies throughout postural perturbations. J. Neurophysiology 107(1):159-177, 2011.

[4] E. Lum, C. Perez, Y. Sun. On detecting and adaptive timing for electromyogram based control signals. Proceedings 38th Northeast Bioengineering Conference, Philadelphia, PA, pp. 43-44, March 16-18, 2012.

[5] S. Suppappola, Y. Sun. Nonlinear transforms of ECG signals for digital QRS detection: a quantitative analysis. IEEE Trans. Biomedical Engineering 41(4): 397-400, Apr. 1994.

Instrumentation for Cell Capacitance Measurements

Switching Sinusoidal Excitations for Studying Cell Membrane Transport

Joseph Cullen, Prashil Patel, Julia Shannon, Eugene Chabot, PhD, Ying Sun, PhD
Department of Electrical, Computer and Biomedical Engineering, University of Rhode Island
Kingston, RI 02881, USA

***Abstract*— This project aims at the design of new instrumentation techniques for studying the electrical properties of the cell as a means of better understanding the cellular transport processes. The approach is to integrate the concept of a lock-in amplifier on a single-electrode platform. Switching sinusoidal excitations can be used to assess small but measurable changes of cell capacitance, which can be used to make inferences about cell surface area changes during the transport processes. In this study, a cell membrane model circuit has been simulated in software. In addition, a proof-of-concept instrumentation has also been implemented with an embedded system. The results have shown the feasibility of obtaining accurate real-time measurements of the cell capacitance by time-multiplexing the sinusoidal excitation and the voltage measurement via a single patch-clamp electrode.**

***Keywords*— cell capacitance; instrumentation; signal processing; cell membrane transport; simulation; embedded system**

I. Introduction

For years scientists have wanted to gain a deeper understanding of the cell's chemical behaviors. More specifically, how often do cells endocytize or exocytize substances? Is it possible to map these processes when they occur? Based off of the finding that cellular capacitance is directly proportional to cell surface area, we have a way to observe these processes. When cell membrane transport occurs, the surface area across the cell increases, which in turn increases the capacitance of the membrane [1]. This can be exploited by the fact that capacitance can be calculated from the phase shift between two signals [2]. So, calculating the phase delay between the input and the output signals in a circuit simulating the electrical properties of a cell membrane can give insight into the cell capacitance. The primary hardware used for these measurements is a sensitive patch clamp amplifier, a source for the stimulus signal, and a phase sensitive detector. The purpose of this study is to determine the effectiveness of a new and innovative method for the patch clamp. The stimulus signal is modeled as a pulse wave amplitude modulated by a sinusoidal wave envelope, which signifies current injection and simultaneous capacitance measurements in the circuit.

II. Methods

In order to effectively test the capacitive measurement technique, a software and hardware simulation of the signals was created. The input and output measurements and trends after using the signal to drive the circuit modeling a cell membrane were observed.

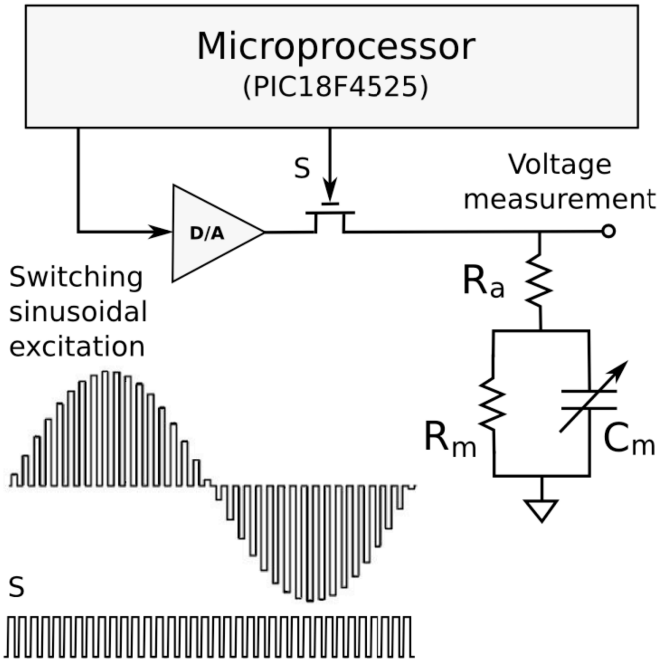

Fig. 1. Schematic diagram of the hardware simulation system for cell capacitance measurements. The cell membrane is modeled by a 3-element RC circuit. The microprocessor generates a switching sinusoidal excitation, which is time-multiplexed with the voltage measurement via a MOSFET switch controlled by the S signal.

A. Software Simulation

The software simulation of the circuit model was done using Simulink (Mathworks, Natick, MA). A pulse wave amplitude-modulated by a sine wave represents the switching sinusoidal excitation shown in the hardware block diagram in Fig. 1. A switching signal (S) is used to turn on the MOSFET switch during the duty cycle of the sinusoidal excitation. The MOSFET is turned off when the pulse wave returned to zero to prevent momentary discharging of the capacitor (C_m). In this simulation, the values for the 3-element cell membrane model were chosen as follows: access resistance R_a = 500 KΩ, rans-membrane resistance R_m = 5 MΩ, and membrane capacitance C_m = 10 pF. The actual parameter values for live cells vary over a broad range depending the types of cells. A report suggests that a typical cell has Ra = 20 MΩ, Rm = 1000 MΩ, and Cm = 5pF [3].

B. Hardware Implementation

Based on the software simulation a proof-of-concept instrumentation system was built. The hardware system was developed with a microprocessor (PIC18F4525, Microchip,

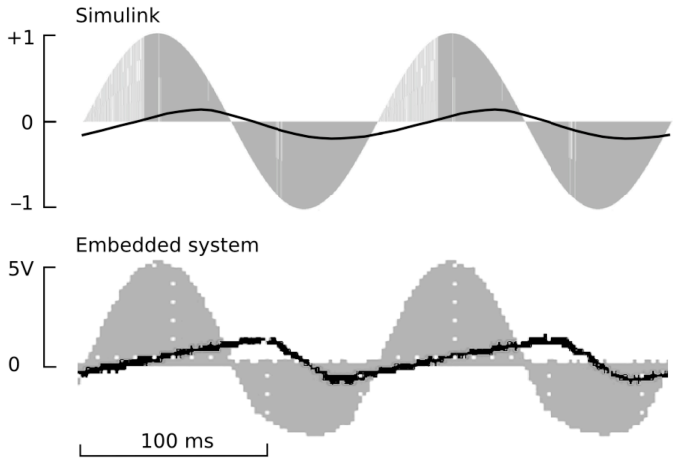

Fig. 2. The switch sinusoidal excitation (grey) and the measured voltage waveform (black) from the software simulation (top) and the embedded instrumentation system (bottom).

Chandler, AZ). As shown in Fig. 1, the embedded system generates the sinusoidally modulated pulse wave and the switching signal (S) to drive the MOSFET switch. The only difference between the software simulation and the hardware implementation was the resistor and capacitor values in the circuit. Some extremely high resistor values or low capacitor values could not be obtained in hardware simulation due to supply constraints. Component values were scaled to commonly available values. Although these components were changed, the time constant for both circuits was kept uniform. In addition, the clock of the PIC18F452 microprocessor was slower than the desirable frequency in the software simulation. Thus, a slower pulse wave frequency was used on the hardware platform.

III. Results

As shown in Fig. 2, the switching sinusoidal excitation was able to induce a sinusoidal response with a phase shift in the voltage measurement. This was observed in both the software simulation and the hardware implementation. The phase shift was comparable: about 40° in the software simulation and about 50° in the hardware implementation. In addition, both of the input and output signals match the simulation model, despite a slight distortion of the input signal in the hardware implementation due to the excessive current drawn by the MOSFET.

In the software simulation (Fig. 2 top), the signals more closely match the cell membrane capacitance models, due to the ideal component models in software. However, because the hardware and the software display the same characteristics and a phase shift roughly equal to the expected phase shift (45°), these results are consistent.

IV. Conclusion

The overall goal of this research was to assess the capacitance in a cell membrane model based a phase shift in the induced voltage in response to a sinusoidal excitation. The significance of this project lies in the combination of the lock-in amplifier concept [4] and the patch clamp technique with a single electrode [5]. The lock-in amplifiers are useful for measuring small signals under noise conditions. The sinusoidal modulation and demodulation process can significantly improve the single-to-noise ratio by rejecting noise outside the very narrow frequency band of the signals. However, a lock-in amplifier usually requires two ports: one for input and one for output. Thus, the traditional lock-in amplifier instrumentation does not lend itself to a patch clamp setting where a single electrode is used to access the cell. This project provides a solution to the application of the lock-in technique to the single-electrode setting. By using a switching sinusoidal excitation, it is possible to time-multiplex current injection and voltage measurement on a single electrode while introducing a sinusoidal modulation. The feasibility of the approach has been demonstrated in this study with the observation of a phase-shifted sinusoidal induced voltage of the same frequency.

Another advantage of the approach lies in the use of a single sinusoidal excitation. Previously reported methods for measuring cell capacitance often require multi-frequency excitations [6] or non-sinusoidal excitations [7]. Furthermore, with a fast digital signal processor it is possible to deliver a cycle of the switching sinusoidal waveform within a relatively short time interval (on the order of 0.1 ms). Thus, this technique will provide a high temporal resolution, which is essential for real-time monitoring of exocytosis and endocytosis activities occurring on the order of 1 ms.

For future work, estimation algorithms will be developed to measure the cell capacitance based on the magnitude and phase of the induced voltage in response to the switching sinusoidal excitation. Additional simulation work will be carried out to assess the accuracy of measuring small cell capacitance changes on the order of 1 fF due to vesicle transports across the cell membrane.

References

[1] F. Schweizer. Capacitance measurements. http://schweizerlab.org/capacitance-measurements, 2013.

[2] S.F. Lempka, D.W. Barnett. Optimization of multi-frequency techniques used for cell membrane capacitance estimation. Proc. 26th Ann. Int. Conf. IEEE EMBS, San Francisco, CA, USA, pp. 522-5, Sep. 1-5, 2004.

[3] S. Misler, D.W. Barnett. An optimized approach to membrane capacitance estimation using dual-frequency excitation. Biophys J. 72: 1641-1658, 1997

[4] M. L. Meade. Lock-in amplifiers principles and applications. P. Peregrinus, 1983.

[5] O.P. Hamill, A. Marty, E. Neher, B. Sakmann, F.J. Sigworth. Improved patch-clamp techniques for high-resolution current recording from cells and cell-free membrane patches. Pflügers Archiv European Journal of Physiology 391 (2): 85–100, 1981.

[6] B. Rituper, A. Gucek, J. Jorgacevski, A. Flasker, M. Kreft, R. Zorec. High-resolution membrane capacitance measurements for the study of exocytosis and endocytosis. Nature Protocols 8(6): 1170-83, 2013.

[7] R.E. Thompson, M. Lindau, W.W. Webb. Robust, high-resolution, whole cell patch-clamp capacitance measurements using square wave stimulation. Biophys J. 81(2): 937-948, 2001.

Medication Reminding Activity Analyzer for Guided Independent Living Environments (MRAAGILE)

Implementing Motion Dependent Medication Reminders

Alexander Batrakov[1], Patrick Merida[1], Nathan Bartels[1], Eugene Chabot[1], PhD,
Patricia Burbank[2], DNSc, RN, Ying Sun[1], PhD
[1]Department of Electrical, Computer and Biomedical Engineering, and [2]College of Nursing, University of Rhode Island
Kingston, RI 02881, USA;

***Abstract*—The MRAAGILE is a device designed to monitor and reinforce medication consumption as well as promote a healthy daily regimen for those who choose to live independently. The device provides interactive reminder messages to inspire the user to follow directives. The purpose of this is to implement motion detection following a reminder to determine whether the user is responding. The device will receive instructions from the user manually on the device or by using a bluetooth wireless link to transmit the times for which medication is to be taken. After reminders are set, the mobile device will continue to function until the first reminder time is reached. A message will be played. If motion is detected, it will serve as an indicator that the message was acknowledged. If not, it will trigger an alarm to remind the user to complete the action. The alarm will deactivate once motion is detected. This device will be useful for increasing the independence for older adults who live in the community as well as assistive living environments.**

***Keywords*—medication reminder; embedded design; activity monitor; voice record/playback; independent living**

I. Introduction

Medication reminders play an important role in promoting independent living. The likelihood of an individual over the age of 60 adhering to medication distribution times is 26-59% [1]. While many people can rely on their short term memory to keep track of the times to receive medication, others do not have that luxury.

The implementation of these reminders typically includes reminders on a PC or TV, or some medium they spend large amount of time in front of [2]. Mobile phones are also good targets since they are easy to carry at all times.

Medication reminders on the market today all share a common flaw: the device does not benefit the user if the reminders are not noticed or prematurely acknowledged and subsequently forgotten. This is especially prevalent in those with impaired cognitive abilities which have problems with short term memory.

The purpose of our modifications is to couple monitoring of the time to a motion detector. This will mean that once the time for medication has been reached and the reminder will trigger, an alarm will be trigger if the user fails to take motion. This is especially geared toward the situation of an individual who leads a sedentary lifestyle, which is becoming increasingly common, and who frequently puts off moving and eventually forgets why they were supposed to move in the first place. The alarm will deactivate once motion has been detected and the device will await the next reminder.

II. Methods

A. Hardware

This wearable device has been developed with an embedded processor (PIC18F4525, Microchip, Chandler, AZ). A 3-dimensional accelerometer (STMicroelectroinics LIS302SG) is used to detect motions and to assess the intensity of activities. Currently, any motion in any axis will deactivate the alarm. A voice record/playback integrated circuit chip (Nuvoton ISD 1750PY) is used to store messages, record new messages, and playback the reminder messages. The mobile device uses a 9 Volt battery as a power source. Presently, the device allows for 6 messages for different reminders and a default alarm. A microprocessor monitors the time for reminder activation, controls the voice chip, and provides action log recording and extraction. The user interface includes two push buttons and an LCD character display to show current time and to confirm the unit is active during the *monitor* mode. During the *program* mode, the user (usually a care-giver or a relative) is able to set the alarm times and enter the voice instructions via the user interface.

B. Device Design

The Activity Analyzer with voice-Guidance for Independent Living Environments (AAGILE) is an ongoing project at the University of Rhode Island [3], [4]. One difference from the previous prototype [5] is adding the medication reminders (MR) instead of only having messages being played after extended periods of inactivity. Also, having the alarms be deactivated by using the accelerometer is also a new feature. Thus, the present project is named MRAAGILE.

Using two buttons on the device to scroll and select, the user will input the time for the Alarm (repeated as many times as needed to cover all medication taken). This data is stored in the PIC processor. The time will be monitored on the mobile unit and will trigger an alarm once the first alarm time has been reached and play until motion is detected. It will then reverence the voice chip and play the message or alarm chosen. Once motion is detected, the alarm will turn off and await the next scheduled alarm.

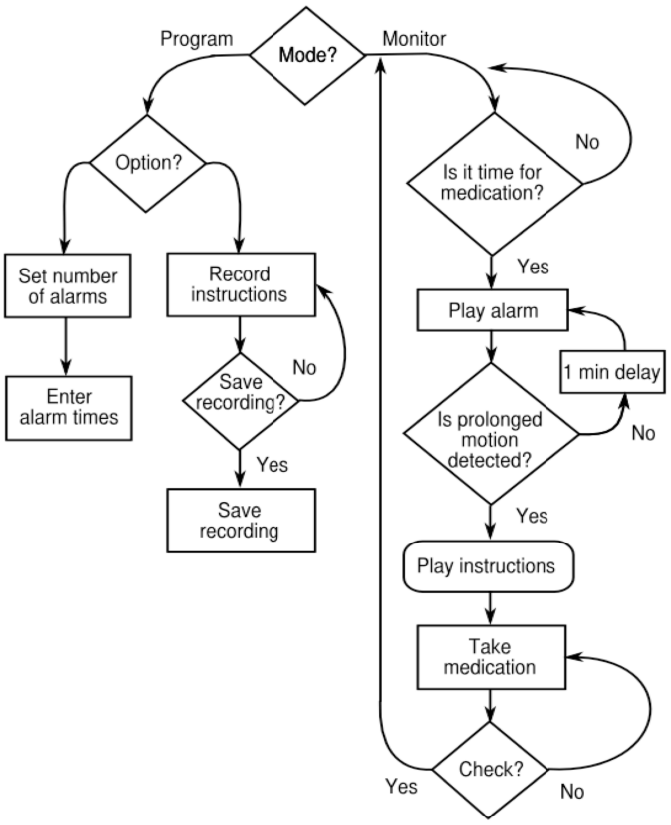

Fig. 1. Flowchart of the medication reminder with pre-recorded voice instructions.

As shown by the flowchart in Fig. 1, if the unit is being programmed, it will allow the user to set alarms and the type of medication that is to be taken for that allotted time. Otherwise, the program will monitor the time to see if an alarm time has been reached, then initiate an alarm. After motion is detected, it will deactivate that alarm and wait for the following alarm time.

III. Results

The device was initially implemented on a breadboard using a 9V rechargeable battery. After successful debugging and optimization, an engineering prototype was built with point-to-point soldering and encased in an ABS plastic box as shown in Fig. 2. The device was placed in a fanny pack and worn around the waist. The preliminary test has shown that MRAAGILE is capable of playing back pre-recorded voice messages at the pre-programmed times according the specifications.

IV. Discussion

The project has resulted an embedded device that provides reminders and voice instructions for daily medications. While many medication reminders are commercially available nowadays, ranging from labeled plastic containers to electronic message reminders, MRAAGILE has the advantages of its activity sensor and voice recording/playback capability. The

Fig. 2. Engineering prototype of MRAAGILE.

effectiveness should be increased by using the activity sensor as a feedback on whether the instructions are followed. In addition, a previous study [6] has shown that voice messages from known persons, especially the loved ones, are most effective to encourage the old adults.

Limitations of the present prototype include the following: First, the mobile unit's button can be inadvertently pressed. Second, the sound of the mobile unit may be too quiet to hear if the messages are played in a very noisy environment.

In addition to the older adult population, this Application should be useful for outpatients who are on medication, and can be programmed by a nurse or family member if the patient is unable to do so himself. Potential future uses of the device would be implementing it solely as an application for the android device and utilizing the accelerometer and processor, and with an internet connection, adding links to more information about medication being inputted and checking whether the amount being administered is in a dangerous range.

References

[1] Y.S. Lee, J. Tullio, N. Narasimhan, P. Kaushik, J.R. Engelsma, S. Basapur. Investigating the potential of in-home devices for improving medication adherence, Pervasive Computing Technologies for Healthcare, 2009. PervasiveHealth 2009. 3rd International Conference pp.1,8, 2009.

[2] E.J. MacLaughlin, C.L. Raehl, A.K. Treadway, T.L. Sterling, D.P. Zoller, C.A. Bond. Assessing Medication Adherence in the Elderly. Drugs & Aging 22 (3): 231–55, 2005.

[3] H. Greene, C. Dulude, A. Neves, Y. Sun, P.M. Burbank. Performance Evaluation of the Activity Analyzer. 38th Annual Northeast Bioengineering Conference, Temple University, Philadelphia, PA, March 16-18, 2012.

[4] K. Rafferty, T. Alberg, H. Green, Y. Sun, P.M. Burbank. Development of an Activity Analyzer with Voice Directions for Exercises. 38th Annual Northeast Bioengineering Conference, Temple University, Philadelphia, PA, March 16-18,2012.

[5] T. Wang, J. Harvey, Y. Sun, E. Chabot. Activity Analyzer for Guided Independent Living Environments (AAGILE). 39th Annual Northeast Bioengineering Conference, Syracuse University, Syracuse, NY, April 5-7, 2013.

[6] P.M. Burback, D. Riebe. Promoting Exercise and Behavior Change in Older Adults: Interventions and Transtheoretical Model. NY: Springer, 2002.

A Microprocessor-Based Wrist Pulse Simulator for Pulse Diagnosis in Traditional Chinese Medicine

Steven McLellan[1], Christina Liese[1], Melissa Andrews[1], Mona Boudreaux[2], G.F. Boudreaux-Bartels[1], Eugene Chabot[1], & Ying Sun[1]
[1]Department of Electrical, Computer, and Biomedical Engineering,
University of Rhode Island, Kingston, RI 02881-0805 USA
[2]A Time to Heal, Wonder Lake, IL 60097 USA

***Abstract*— Pulse diagnosis has been an important practice in traditional Chinese medicine for diagnosing various diseases. It is based on the patterns of blood pressure pulses at the wrist felt with three fingers. The device developed in this study mimics the outward forces generated by blood flow patterns through the radial artery. The embedded system platform allows for the implementation of various pulse patterns in response to the depression pressure of the fingers. The resulting pulse simulator is useful for demonstrating and teaching the art of pulse diagnosis.**

Keywords*— *pulse diagnosis; simulator; pulse patterns; blood pressure; traditional Chinese medicine

I. Introduction

The ability to diagnose a disease based on the arterial pulse patterns that can be felt in the wrist is a method often referred to as pulse diagnostics originating from the traditional Chinese medicine. In the area of pulse diagnostics, as many as 29 patterns have been identified and related to diagnosis of a wide range of diseases and conditions [1],[2]. These range from detecting liver and gall bladder diseases to detecting pregnancy [3]. In order to distinguish between these patterns, six characteristic qualities of the wrist pulse patterns have been defined including pulse width, depth, strength, rate, length, and rhythm [4]. The detection of these pulse patterns requires the use of three fingers (index, middle, and ring fingers) placed over the radial artery at the wrist of the subject. Three different pressures (light, medium, and high) are applied to the artery to reveal different responses [5].

Despite the relatively large number of pulse patterns, frequently encountered patterns are fewer than 10. Thus, some of the rarely encountered pulse patterns are difficult to demonstrate. The purpose of the presented work is to create a device that simulates the pulse patterns for the purposes of demonstrating and teaching the art of pulse diagnosis.

II. Methods

A. Device Design

As shown by the block diagram in Fig. 1, the mechanical part of the system consists of three solenoids presenting the pulse waveforms to the three fingers that feel the pulses. The electronic part of the system consists of a microprocessor that outputs the stored digital pulse waveforms to the solenoids via three digital-to-analog (D/A) converters. A pressure sensor detects the gripping forces applied to the simulator. The pressure is sensed by the microprocessor and evokes different responding pulse waveforms. As shown by the schematic diagram in Fig. 2, the overall device is composed of two subunits connected via a cable. One enclosure contains the solenoids in a stable position creating an artificial wrist model made of silicon. The wrist model has a pressure sensor at the base for the user to apply pressure with their thumb while measuring the wrist pulse. When more pressure is applied with

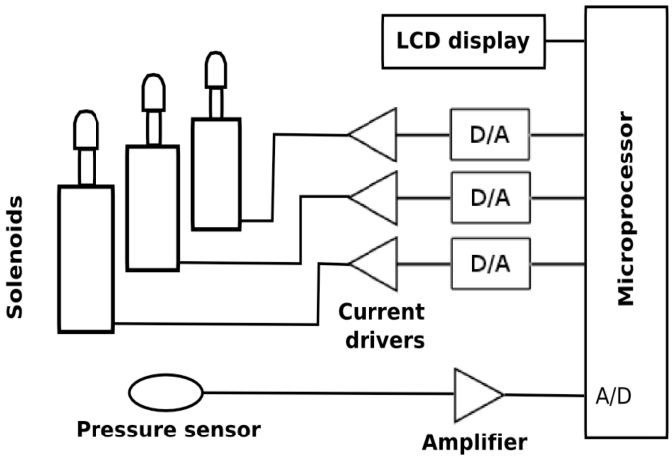

Fig. 1. Block diagram of the pulse simulator.

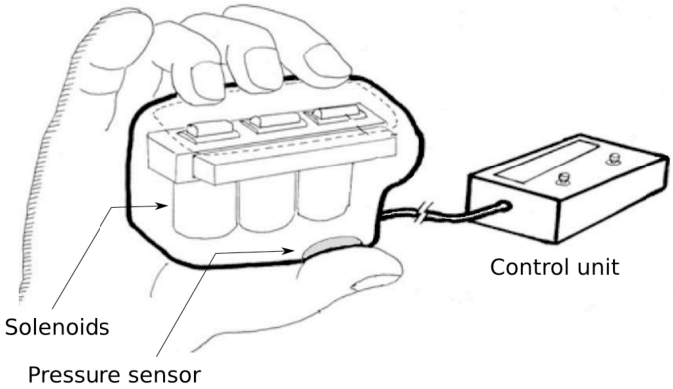

Fig. 2. Schematic diagram of the pulse simulator.

the thumb, the pulse either increases or decreases in strength which varies with the selected mode. The user places three fingers, as is the standard practice for pulse diagnostics, to measure the pulse characteristics. The pistons of the solenoids generate forces corresponding to the pulse waveforms through a thin layer of the encasing silicone rubber. A second component is the control unit that provides user interventions through a LCD display and push buttons. The control unit also contains the microprocessor, the electronics, and a battery power source.

B. Pulsatile Waveform Generation

The microprocessor based system manipulates a series of solenoids creating the pulses of these waveforms. Of the six pulse characteristic quantities, the pulse width is related to the width of the artery, which is not represented in the current system. The strength is represented by the stroke distance of the solenoid's piston. The pulse depth is represented by varying the waveforms in response to the applied pressure measured with the pressure sensor. The rate is controlled by the microprocessor, which sets the playback sampling frequency of the stored digital waveforms. The length represents the duration of one pulsation, which is controlled by the duty cycle of the stored waveforms and the playback frequency. The rhythm is represented by the irregularity of repeating the playback waveform. A condition of irregular rate (arrhythmia) can be introduced by randomizing the playback frequency each time the waveform corresponding to a cardiac cycle is repeated.

C. Hardware and Software

The pulse simulator system was developed by use of a PIC microprocessor (PIC18H4525, Microchip, Chandler, AZ). The software was coded in the C language using the MPLab development tool (Microchip, Chandler, AZ). The software algorithms include the retrieval of pulse waveforms from lookup tables, a real-time playback engine driven by timer interrupts, the applied pressure measurement via the on-chip analog-to-digital converter, and schemes for varying the pulse magnitudes and playback rates.

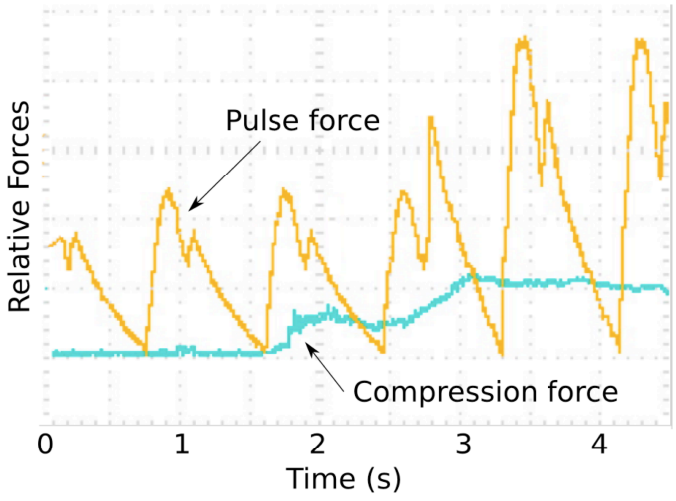

Fig. 3. Playback pulse waveform (orange) was altered by the compression force (blue) detected by the pressure sensor.

III. Results

The hardware and software of the pulse simulator system have been successfully implemented. The force waveforms generated by the solenoids resemble the actual pulses felt at the wrist. As shown in Fig. 3, the pulse waveforms can be programmed to respond to the applied pressure in a dynamic way. For this example, the magnitude of the pulse waveform increases in response to an increase in the gripping pressure. This represents a typical pulse pattern of a healthy subject that shows an increase in strength when the fingers are pressed down harder on the radial artery.

For the current implementation, a total of three different force waveforms are implemented, which include a normal depth pulse, a deep pulse, and a floating pulse. The same waveform is applied to all three solenoids but with a delay of 1 ms between adjacent solenoids. For rate variations a total of four rhythms are implemented, which include normal heart rate, bradycardia, tachycardia, and arrhythmia. Thus, the current system can switch among 12 different pulse patterns (3 waveforms x 4 rhythms). For the normal depth pulse, there is a maximum amplitude at mid-range pressure. The superficial or floating pulse has a maximum amplitude at low pressure and the deep pulse has a maximum amplitude at higher pressure. The user interface allows for the selection of the playback pattern, which is shown on the LCD display.

IV. Discussion

In this study an instrument has been developed to simulate the wrist pulse patterns used in the pulse diagnosis of the traditional Chinese medicine. The project has resulted in an embedded system that produces three force waveforms via three solenoids in response to the applied gripping pressure. The playback rate of the waveforms can also be programmed to reflect either normal or abnormal heart rhythms. To our knowledge, this is an innovative device that provides a unique opportunity for training practicians of pulse diagnostics.

Future work is planned to implement additional pulse diagnostic characteristics including frail, wiry, rolling, and choppy pulses through software modifications. In order to address the pulse width characteristic, further hardware design changes are necessary as the current design utilizes fixed-size pistons. Improvements on the user interface are also considered to show the pulse waveforms on a graphic LCD display and to provide more descriptive information about the pulse patterns.

References

[1] S. Walsh, E. King. Pulse Diagnosis: A Clinical Guide. 1st edition. Publisher: Churchill Livingstone. December 2007.

[2] B. Flaws. The Secret of Chinese Pulse Diagnosis. 2nd edition. Boulder, CO: Blue Poppy Press. March 1997. Wiley.

[3] A. Stone. Pulse diagnosis made ridiculously simple. Retrieved from TCM TV. http://HealthStream.tv, February 23, 2010.

[4] G. Maciocia, S.X. Ming. Pulse Diagnosis in The Foundations of Chinese Medicine, China, Elsevier, 2005.

[5] Diagnostics of Traditional Chinese Medicine. Xue Yuan Academy Press, 2002.

Time Dependent Skin Impedance Model

For the testing of electrocutaneous stimulating electrodes

Courtney Medeiros, Christopher Ross DeSanto, Ryan McDonough, Eugene Chabot, and Ying Sun
Department of Electrical, Computer, and Biomedical Engineering, University of Rhode Island
Kingston, RI 02881-0805 USA

***Abstract*—Skin resistance changes dynamically during the time course of an external electrical stimulation. An embedded system was developed to provide a dynamic impedance in response to external stimulations. A microprocessor adjusts the series resistance component of an impedance based on a preprogrammed function. This skin impedance model is useful for testing devices involving electrocutaneous stimulation or functional electrical stimulation.**

Keywords—skin impedance; electrocutaneous stimulation

I. Introduction

Electrocutaneous stimulation passes current through the epidermis and dermis to evoke tactile sensations. The purpose of this model is to enhance the common resistor-capacitor (RC) skin impedance model to encompass the temporally variable impedance after the onset of electrocutaneous stimulation. The developed model extends the first-order skin model described by Polleto [1] to include a time dependent resistance measured by Mason [2].

Current and past electronic tissue models for electro-cutaneous stimulation focus on the fluctuation of skin resistance as a function of frequency. The purpose of this model is to enhance the common resistor-capacitor (RC) skin impedance model to encompass the temporally variable impedance after the onset of electrocutaneous stimulation. The developed model extends the first-order skin model described by Polleto [1, 3-5] to include a time dependent resistance measured by Mason [2]. The model employed in the present study expands on the first-order skin model described by Potello [1, 3-5] by adding a comparator for monitoring the time course of the external electrical stimulation. At the onset of a stimulation, a microprocessor initiates a program and a digital potentiometer to account for the temporal variance in impedance.

II. Methods

A. Device Design

As shown by the block diagram in Fig. 1, a first-order skin impedance model consists of three elements: a serious resistance (R_s), a parallel resistance (R_p), and a capacitance (C). While the skin resistance values of the electrode/skin interface vary greatly, as reported by Poletto [4], a value of 320 KΩ was selected for R_p and a 0.42 nF for C in the present model. The time-varying component is attributed to the series resistance R_s, which is implemented with a digital Potentiometer. The digital potentiometer (MCP4162,

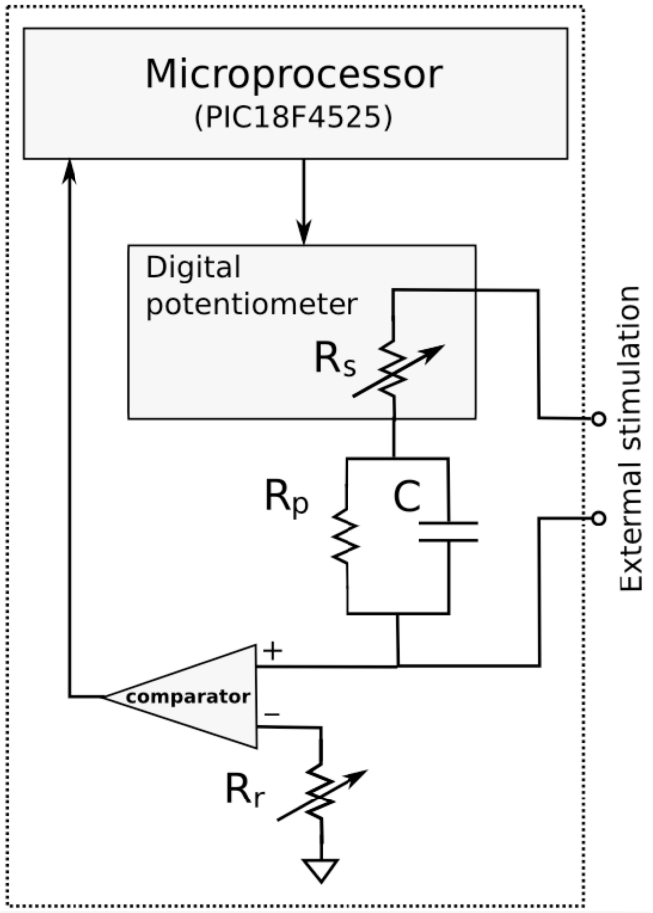

Fig. 1. Block diagram of the microprocessor based skin impedance model.

Microchip, Chandler, Arizona) is responsible for varying the series resistance consistent with Mason's results over the desired range of 24 KΩ to 27.5 KΩ.. A microprocessor (PIC18F4525, Microchip) selects one of the 69 different resistance values over a duration of 90 s from a look-up table.

To derive the values for the look-up table of, an estimate of the resistance values were obtained from Mason's published results [2]. With theses results, R_s is approximated by the following function:

$$R_s = 12500\, t\, e^{-t} + 23000\ \Omega \quad (1)$$

where t is the elapsed time in seconds since the onset of an external stimulation. The desired time course of R_s is shown in Fig. 2.

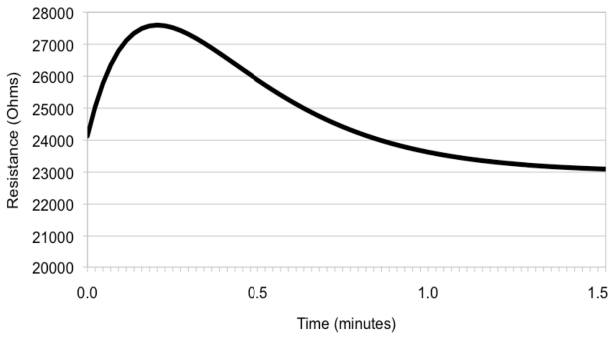

Fig. 2. Desired series resistance (R_s) based on equation (1).

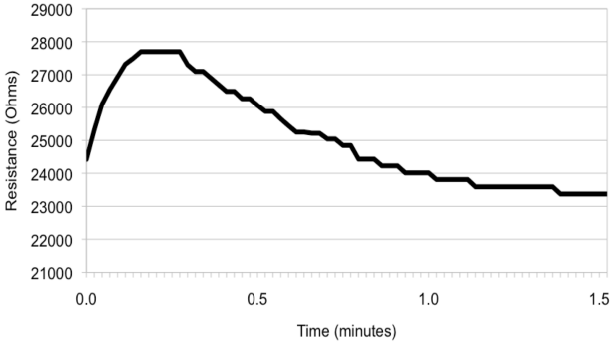

Fig. 3. Measured series resistance (R_s) from the skin resistance model.

B. *Electrode Sensing*

In order to make this model dependent on the onset of electrocutaneous stimulation, the embedded system incorporates a comparator that triggers upon the application of an external stimulus voltage. Once the comparator reads the applied stimulus voltage to be greater than the threshold voltage, the microprocessor initializes the generation of the skin response in the program. An interrupt-driven timer in the microprocessor keeps track of the real time. Values from the look-up table are sequentially outputted to the digital potentiometer to set the appropriate resistance as time elapses. If the end of the look-up table is reached, the last resistance value is maintained to mimic the homeostatic numbing response of the skin. The microprocessor will only reinitialize the array sequence when the present stimulus is removed followed by the detection of another stimulus. This specific function of the model allows for consecutive testings of electrocutaneous stimulation.

III. Results

The hardware was built according to the model presented above and the software was coded in the C language using the MPLab development tool (Microchip, Chandler, AZ). The system has demonstrated to respond to an applied stimulus according to the specifications. At the onset of a stimulus event generated with a function generator, the skin impedance progresses through the desired level changes as shown in Fig. 3. The system correctly restarts upon the removal of the applied stimulus.

IV. Discussion

This study has resulted in an embedded system that mimics the dynamic impedance properties of the skin in response to electrocutaneous stimulation. Compared to other skin models that focus on the variable change of skin resistance versus frequency, the presented approach has enhanced the model to include the temporal change of the skin impedance during the course of an stimulation episode.

This novel device can be used for testing electrocutaneous stimulation, which provides tactile sensation. By creating a dynamic skin impedance model, electrocutaneous stimulation devices can be evaluated in terms of their ability to adjust the desirable stimulation currents under a time dependent load. This skin impedance model can also be used to test functional electrical stimulation devices. The programmability of the model makes it very flexible for implementing different time courses of the impedance changes.

The limitations of the present model include the following. The output doesn't perfectly match Mason's data [2]. In reality there may exist a delayed response to the external stimulation. The onset of the waveform does not trigger on the electrode application to the skin, which is what Mason stated as his time 0. The accuracy of the time dependent resistance might be improved by increasing the size of the look-up table. This model is also limited because it assumes that only the series resistance (R_s) changes over time.

Future work on this model can be performed to examine the impact of time on the frequency response. Exploring the effects of skin moisture and environmental humidity on baseline skin resistance can make another addition to this model.

References

[1] Poletto, C. J., & Van Doren, C. L, "A High Voltage, Constant Current Stimulator for Electrocutaneous Stimulation Through Small Electrodes," IEEE Trans. Biomed. Eng., vol. 46, pp. 929-936, 1999. Kaczmarek, K.A., Kramer, K.M., Webster, J.G. and Radwin, R.G, "A 16-Channel 8-Parameter Waveform Electrotactile Stimulation System". IEEE Trans. Biomed. Eng., vol. 38, pp. 933-943, 1991.

[2] Mason, J.L., & MacKay, N.A.M, "Pain Sensations associated with Electrocutaneous Stimulation," IEEE Trans. Biomed. Eng., vol. 23, pp. 405-409, 1976. Kaczmarek, K. A., & Webster, J. G, "Voltage-Current Characteristics of the Electrotactile Skin-Electrode Interface," in Proc. 11th Annu. Int. Conf. IEEE Eng. Med. Biol. Soc., Seattle, vol. 11, pp. 1527, 1989.

[3] Kaczmarek, K. A., & Webster, J. G, "Voltage-Current Characteristics of the Electrotactile Skin-Electrode Interface," in Proc. 11th Annu. Int. Conf. IEEE Eng. Med. Biol. Soc., Seattle, vol. 11, pp. 1527, 1989.

[4] Kaczmarek, K.A., Kramer, K.M., Webster, J.G. and Radwin, R.G, "A 16-Channel 8-Parameter Waveform Electrotactile Stimulation System". IEEE Trans. Biomed. Eng., vol. 38, pp. 933-943, 1991.

[5] H. C., Young, S. T., & Kuo, T. S, "A Versatile Mutlichannel Direct-Synthesized Electrical Stimulator for FES Applications," IEEE Trans. Instrum. Meas., vol. 51, pp. 2-8, 2002.

An Upper Airway Model for Studying the Acoustic Properties of Breathing Sounds

Andrew McNaught, Connor Walsh, George Douleh, Ying Sun, PhD, and Eugene Chabot, PhD

Department of Electrical, Computer and Biomedical Engineering
University of Rhode Island, Kingston, RI 02881-0805 USA

***Abstract*—The acoustics of the upper airway may provide useful insights to medical conditions such as snoring and obstructive sleep apnea. This study is intended to create an artificial airway model that has acoustic properties similar to those of the humans. A silicone rubber head model with anatomically correct nasopharynx, oropharynx, and trachea was built. A respiration pump was used to drive air in and out of the airway, simulating inhalation and exhalation of the human respiratory cycle. Measurements were taken by use of an electronic stethoscope positioned near the area of the suprasternal notch. Frequency spectra showed an increased in high frequency components when the trachea was blocked by about 90%. The silicone head model provides a controlled environment for studying the effects of blockages at various part of the upper airway on the acoustic properties of the breathing sounds.**

Keywords— silicone head model; upper airway; breathing sound; frequency spectrum;

I. INTRODUCTION

Sleep apnea is an under diagnosed disease that has gained much attention in recent years. The collapsed airway causes momentary pauses in breathing during sleep, which often interrupts the deep sleep stage. and this causes the brain to send a signal to wake up due to the lack of air intake in the lungs. Abruptly waking up from a deep sleep may increase the risk of heart attack, stroke, and other heart related issues [1]. To aid the diagnostics of sleep apnea, our laboratory has conducted research on the acoustic properties of the breathing sounds in relation to obstructions in the upper airway.

The current project looks to the characterization of frequency spectrum of a healthy trachea versus that of one which has been obstructed. The project contains two parts. First, a head model that contains a hollow airway needs to be constructed with a single pour of silicone rubber. The silicone model must not includes interfaces that could block the transmission of sounds. Second, the frequency spectra of the airflow sounds created by connecting a respiration pump to the head model are studied. Specifically, the effects of an airway blockage on the frequency spectrum are characterized.

II. METHODOLOGY

A. Overall Instrumentation

As shown in Fig. 1, the breathing is generated by a respiration pump (Harvard Apparatus model 607), which

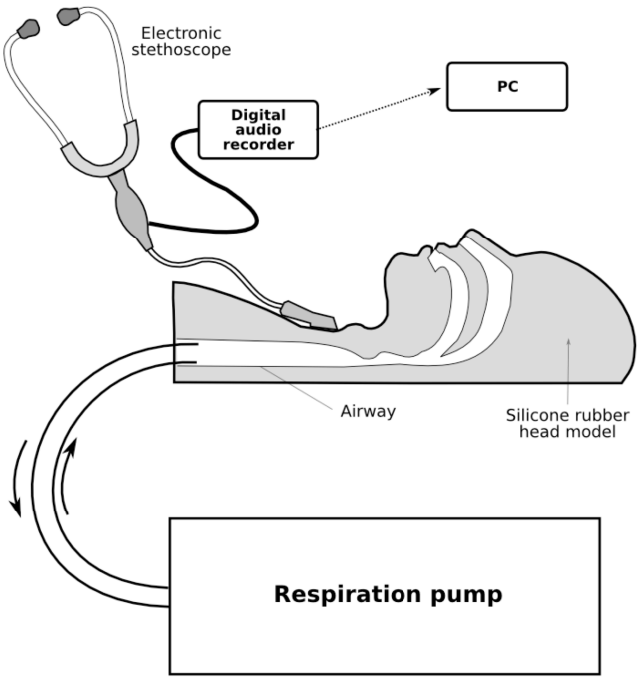

Fig. 1. Silicone rubber head model with attached respiration pump to simulate breathing through the upper airway.

pumps air in and out of the silicone head model. The pump allows for adjustability in the rate of breathing, which is typically set at 18-20 respirations per minute. An minute. An electronic stethoscope (Jabes, GSTechnology, Seoul, Korea) is placed over the trachea near the suprasternal notch. A digital audio recorder (H4N, Zoom Corp., Tokyo, Japan) is attached to the stethoscope and records the airflow sounds. The data are saved as a wav file and uploaded to a personal computer. A MATLAB program performs the fast Fourier transform (FFT) and displays the frequency spectrum.

B. Airway

The techniques for constructing the head model was based on a previous project [2]. To create the airway mold, two blocks of wood were carved and placed together to perfectly match the tracheal dimensions of an adult human. This mold was filled with agar, an algae based substance, with a hardening state stronger than most other types of gelatin. The agar airway model was then placed in a plaster mold of a human head mannequin, anchored

down, and filled with the silicone rubber. After the silicone hardened, the agar was removed from the airway with boiling water. The respiration pump is connected to the airway with pneumatic tubings.

C. Silicone Model

To construct the silicone head model, a silicone mix with 10:1 ratio of the hardener was used. This mixture was first poured in a vacuum container allowing for the removal of air bubbles. The silicone was then poured around the agar, which represented out trachea, and was left to harden. Once the silicon set, the agar was removed by pouring boiling water through the mouth and nose and down the center trachea. Figure 1 shows the final head model with the upper airway void.

III. Results

A. Unobstructed Airway

A number of measurements were taken throughout the testing process. The first round of results looked at mimicking the breathing process of a healthy individual with the silicone model. Measurements were taken using a speed of 18-20 beats per minute on the respiratory machine. As shown in Fig. 2, the frequency spectrum is, to some extent, similar to that of the typical frequency spectrum of the human breathing sound, with a low frequency peak around 100 Hz and high frequency components between 300 Hz and 700 Hz.

B. Obstructed Airway

Next, the main trachea was obstructed by inserting clay into it so that approximately 90% of the opening was blocked. The results in Fig. 3 shows a significant increase in the higher frequency range around 600 Hz.

IV. Discussion

This project has successfully produced a silicone head model containing an anatomically correct upper airway. The preliminary acoustic measurements have shown that the model can product airflow sounds similar to those of human breathing. Furthermore, the frequency spectrum is sensitive to airway obstructions, suggesting its potential for studying the acoustic properties of breathing sounds related to obstructive sleep apnea.

References

[1] Y. Yang. Result Filters. National Center for Biotechnology Information. U.S. National Library of Medicine, n.d. Web. 17 Dec. 2013.

[2] T. Shanker, G. Downe, E. Chabot, Y. Sun. A silicone human head model for testing acoustic properties of the upper airway. 39th Northeast Bioengineering Conference, Syracuse, NY, April 5-7, 2013.

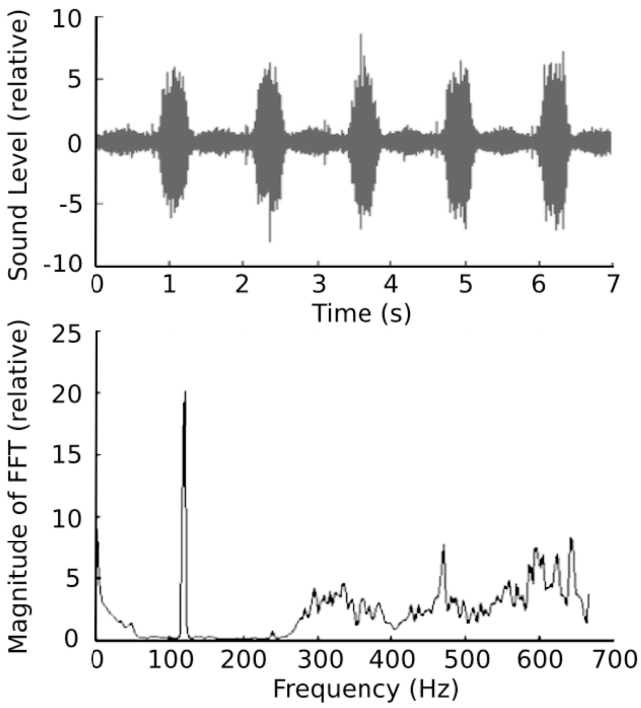

Fig. 2. The airflow sound (top) and the frequency spectrum from an experiment with unobstructed airway

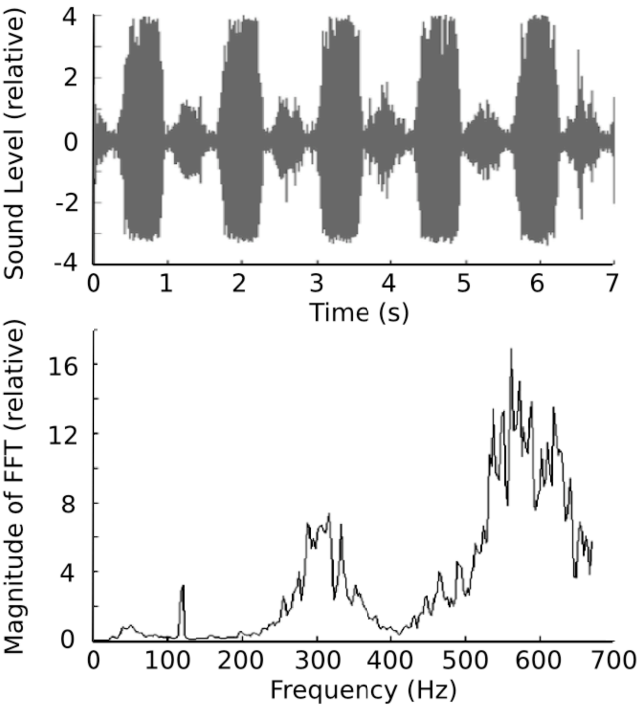

Fig. 3. The airflow sound (top) and the frequency spectrum from an experiment with 90% obstructed airway.